Journal of Genetics and Genomics 46 (2019) 379–387

Contents lists available at ScienceDirect

Journal of Genetics and Genomics

Journal homepage: www.journals.elsevier.com/journal-of-genetics-and-genomics/

Original research

OSBPL2-disrupted pigs recapitulate dual features of human hearing loss and hypercholesterolaemia

Jun Yao [a, b, 1], Huasha Zeng [a, c, 1], Min Zhang [a], Qinjun Wei [a, b, d], Ying Wang [a, b], Haiyuan Yang [a, b], Yajie Lu [a, b], Rongfeng Li [a, b], Qiang Xiong [b], Lining Zhang [b], Zhibin Chen [e], Guangqian Xing [e], Xin Cao [a, b, d, *], Yifan Dai [a, b, *]

[a] Department of Medical Genetics, School of Basic Medical Science, Nanjing Medical University, Nanjing, 211166, China
[b] Jiangsu Key Laboratory of Xenotransplantation, Nanjing Medical University, Nanjing, 211166, China
[c] State Key Laboratory of Reproductive Medicine, Department of Prenatal Diagnosis, Nanjing Maternity and Child Health Care Hospital, Women's Hospital of Nanjing Medical University, Nanjing, 210004, China
[d] The Laboratory Center for Basic Medical Sciences, Nanjing Medical University, Nanjing, 211166, China
[e] Department of Otolaryngology, The First Affiliated Hospital of Nanjing Medical University, Nanjing, 210029, China

ARTICLE INFO

Article history:
Received 12 March 2019
Received in revised form
3 June 2019
Accepted 4 June 2019
Available online 13 August 2019

Keywords:
OSBPL2
Bama miniature pig
Hearing loss
Hypercholesterolaemia

ABSTRACT

Oxysterol binding protein like 2 (*OSBPL2*), an important regulator in cellular lipid metabolism and transport, was identified as a novel deafness-causal gene in our previous work. To resemble the phenotypic features of *OSBPL2* mutation in animal models and elucidate the potential genotype-phenotype associations, the *OSBPL2*-disrupted Bama miniature (BM) pig model was constructed using CRISPR/Cas9-mediated gene editing, somatic cell nuclear transfer (SCNT) and embryo transplantation approaches, and then subjected to phenotypic characterization of auditory function and serum lipid profiles. The *OSBPL2*-disrupted pigs displayed progressive hearing loss (HL) with degeneration/apoptosis of cochlea hair cells (HCs) and morphological abnormalities in HC stereocilia, as well as hypercholesterolaemia. High-fat diet (HFD) feeding aggravated the development of HL and led to more severe hypercholesterolaemia. The dual phenotypes of progressive HL and hypercholesterolaemia resembled in *OSBPL2*-disrupted pigs confirmed the implication of *OSBPL2* mutation in nonsydromic hearing loss (NSHL) and contributed to the potential linkage between auditory dysfunction and dyslipidaemia/hypercholesterolaemia.

1. Introduction

Hearing loss (HL) has become a major health problem affecting 466 million persons globally (6.1% of the world's population), of which 34 million (7.3%) are children (https://www.who.int/deafness/en, accessed 31 October 2018). Genetic factors are responsible for more than half of these cases with congenital HL, as well as for a considerable number of unpredicted postlingual HL cases (Egilmez and Kalcioglu, 2016; Korver et al., 2017; Sheffield and Smith, 2018). Nonsyndromic HL (NSHL) accounts for 70% of hereditary HL, which is commonly caused by monogenic mutations with different inheritance patterns (Cohen and Gorlin, 1995; Dror and Avraham, 2009; Egilmez and Kalcioglu, 2016). Autosomal dominant NSHL (DFNA), accounting for 20%–25% of NSHL cases, has drawn much attention due to its distinct phenotypic characteristics in age-at-onset, progressive rate, severity and frequency (Cohen and Gorlin, 1995; Petersen, 2002). To date, a total of 73 *DFNA* loci have been mapped in the human genome, but only 45 genes have been identified (http://hereditaryhearingloss.org, accessed 10 November 2018). These genes contribute to the precise regulation of intracellular transport, neurotransmitter release, ionic homeostasis, and cytoskeleton maintenance of hair cells (HCs) in the inner ear, which is sensitive to genetic defects that could lead to

Abbreviations: ABR, auditory brain reaction; BC, basic chow; DFNA, autosomal dominant nonsyndromic hearing loss; HC, hair cell; HFD, high-fat diet; HL, hearing loss; IHC, inner HC; MT, mutant; NSHL, nonsyndromic HL; OHC, outer HC; PFFs, porcine foetal fibroblasts; SNHL, sensorineural HL; TUNEL, terminal-deoxy-nucleotidyl transferase dUTP nick end labeling; WT, wild-type.

* Corresponding authors.
E-mail addresses: caoxin@njmu.edu.cn (X. Cao), daiyifan@njmu.edu.cn (Y. Dai).
[1] These authors contributed equally to this work.

https://doi.org/10.1016/j.jgg.2019.06.006

the malfunction/abnormality of the inner ear and the consequent HL.

In our previous study, a novel DFNA-causal gene, oxysterol binding protein like 2 (*OSBPL2*; OMIM: 606731), was identified in a large affected Chinese family via whole-exome sequencing (Xing et al., 2015). Thereafter, the implication of *OSBPL2* in DFNA was also described in an affected German family (Thoenes et al., 2015). It is noteworthy that all affected subjects from the two families carried a heterozygous frameshift mutation in *OSBPL2* and showed mild-to-profound sensorineural HL (SNHL), recapitulating a typical feature in DFNA. OSBPL2, a member of the oxysterol binding protein (OSBP)-related protein (ORP) family, participates in various cellular processes, including lipid/cholesterol metabolism, signal transduction, vesicular transport and cytoskeletal regulation (Laitinen et al., 2002; Suchanek et al., 2007; Hynynen et al., 2009; Sewer and Li, 2013; Escajadillo et al., 2016; Kentala et al., 2018a, 2018b). The potential role of OSBPL2 in hearing function was indicated by the importance of cholesterol homeostasis in the inner ear as well as the unique sensitivity of the auditory organ to changes in cholesterol localization (Evans et al., 2006; Berardino et al., 2007; Helzner et al., 2011; King et al., 2014; Malgrange et al., 2015; Chang et al., 2015; Aghazadeh-Attari et al., 2017). Epidemiologic studies also indicated that hyperlipidaemia/hypercholesterolaemia was predisposed to SNHL (Evans et al., 2006; Helzner et al., 2011; Malgrange et al., 2015; Chang et al., 2015; Aghazadeh-Attari et al., 2017). The implication of *OSBPL2* defects in SNHL makes it an ideal target for investigating the association between the physiopathology of the inner ear and the deregulation of cholesterol homeostasis. Miniature pigs are genetically, developmentally, anatomically, and physiologically closer to humans than rodent animals and other small mammals and carry identical mutations with similar pathogenicity in humans (Bendixen et al., 2010; Prabhakar, 2012; Walters et al., 2012; Prather et al., 2013; Zhou et al., 2015; Chen et al., 2016; Hai et al., 2017a; 2017b; Yan et al., 2018; Yao et al., 2017; Fang et al., 2018). More importantly, the otic structure and function of pigs are more similar to that of humans, which makes miniature pigs a suitable animal model for otology and audiology studies (Lovell and Harper, 2007; Strain, 2015; Guo et al., 2015; Zou et al., 2015).

In this study, CRISPR/Cas9-mediated gene editing was used to mutate *OSBPL2* in porcine foetal fibroblasts (PFFs) derived from Bama miniature (BM) pigs, and then the *OSBPL2*-disrupted PFFs were subjected to somatic cell nuclear transfer (SCNT) and embryo transplantation to generate *OSBPL2*-disrupted piglets. Our results showed that *OSBPL2* disruption could lead to progressive HL and hypercholesterolaemia, which were more severely aggravated in *OSBPL2*-disrupted pigs fed with high-fat diet (HFD). This work will contribute to elucidating the potential pathogenesis of *OSBPL2* deficiency and revealing the potential linkage between SNHL development and hypercholesterolaemia.

2. Results

2.1. CRISPR/Cas9-mediated disruption of OSBPL2 in PFF cells

The porcine *OSBPL2*, which comprises 14 exons and encodes a protein of 468 amino acid residues, is highly syntenic and evolutionarily close to human *OSBPL2* (Figs. 1A and S1). Both porcine and human OSBPL2 proteins have a highly conserved C-terminal OSBP-related domain (ORD) (Figs. 1A and S2), which is specifically found in the OSBP superfamily. It is noteworthy that both reported frameshift mutations in human *OSBPL2* (c.153_154delCT and c.141_142delTG) resulted in prematurely truncated OSBPL2 proteins lacking part of the ORD domain (Fig. S3) and led to HL in affected individuals (Xing et al., 2015; Thoenes et al., 2015), suggesting that the ORD domain is essential for OSBPL2's function. Thus, two sgRNAs separately targeting the exons 5 and 6 (the upstream coding region of ORD) were designed for CRISPR/Cas9-mediated editing of *OSBPL2* (Table S1). The cleavage efficiencies of the two sgRNAs in post-transfected PFFs were determined by T7E1 cleavage assay. The results showed that only the sgRNA targeting exon 5 (sgRNA-exon5) could induce indels in the target region with a cleavage efficiency of 11.4% (Fig. S4; Table S1). Subsequently, the plasmid carrying the *Cas9* and sgRNA-exon5 and the pCMV-td-Tomato plasmid carrying a neomycin-resistance gene were co-transfected into the early passage of primary PFFs. Viable cell colonies were obtained using G418 screening and subjected to genotyping via TA cloning and direct PCR-based sequencing. A total of 34 positive cell clones for sgRNA-exon5 were identified (Table S2). To achieve the faithful effect of *OSBPL2* disruption on auditory function, *OSBPL2*$^{-/-}$ PFF clones were selected for generating *OSBPL2*-disrupted pigs by SCNT and embryo transplantation.

2.2. Generation of OSBPL2-disrupted pigs by SCNT and embryo transplantation and genotypic analysis

Two *OSBPL2*$^{-/-}$ cell colonies were usually pooled in one nuclear transfer, and the reconstructed embryos were transferred to the recipients. Three surrogates developed to term and gave birth to 16 female cloned piglets (Table 1). Among these newborn piglets, 2 were weak after birth and died in 2 weeks. The remaining 14 piglets were born healthy and developed normally (Fig. 1B). The genotypes of cloned piglets were determined by TA cloning and PCR-based sequencing using DNA samples derived from ear tissues. As shown in Fig. 1C and D, 14 cloned piglets carried the expected mutations at the target locus, including 11 *OSBPL2*$^{c.293insT/c.293insT}$ piglets, 2 *OSBPL2*$^{c.293insT/c.284\_291delTCACCGAG}$ piglets and 1 *OSBPL2*$^{c.293insT/c.289\_297delGAGTACATG}$ piglet, which were consistent with the genotypes of the donor cells. Western blot confirmed the disruption of *OSBPL2* in these cloned piglets (Fig. 1E). To assess the off-targeting effect of the CRISPR/Cas9-mediated editing in the cloned pigs, 24 predicted potential off-target sites (OTS) were screened by BLAST (Fig. S5) and DNA sequencing using primers that flanked potential OTS (Table S3). The results showed that no mutations were found in these OTS in the cloned piglets, indicating that the sgRNA-exon5 exhibited a high specificity to the target site in PFFs.

Among the three allelic modifications in cloned piglets, two allelic frameshift mutations (c.293insT and c.284_291delTCACCGAG) resulted in prematurely truncated OSBPL2 proteins lacking part of the ORD domain (p.Tyr98Leufs*231 and p.Thr96Hisfs*230) (Fig. S6A), and one 9-bp deletion mutation (c.289_297delGAGTACATG) led to the absence of 3 amino acid residues in the ORD domain (p.Glu97_Met99del) which might result in the structural alteration and functional impairment of OSBPL2 (Fig. S6B). These allelic mutations in porcine *OSBPL2* might lead to the disease phenotype with similar pathogenicity in humans.

2.3. Effect of OSBPL2 disruption on auditory function in pig models

To provide substantial evidence of the pathogenesis of *OSBPL2* disruption and elucidate the genotype-phenotype association, the mutant (MT) piglets were subjected to phenotypic characterization at varying ages. The high-fat diet (HFD) was introduced as the risk factor for hyperlipidaemia/hypercholesterolaemia implicated in NSHL development. As the two *OSBPL2*$^{c.293insT/c.284\_291delTCACCGAG}$ piglets and one *OSBPL2*$^{c.293insT/c.289\_297delGAGTACATG}$ piglet were insufficient to be sorted, only the 11 *OSBPL2*$^{c.293insT/c.293insT}$ piglets were divided into basic chow (MT-BC, $n = 5$) and HFD (MT-HFD, $n = 6$) groups and subjected to subsequent investigations. Age-

Table 1
Summary of *OSBPL2*-disrupted piglet generation.

Recipient	Fused and transferred embryos[a]	Piglets (born/living)	Live-born piglets with differential genotypes		
			c.293insT/c.293insT	c.293insT/c.284_291delTCACCGAG	c.293insT/c.289_297delGAGTACATG
OSP-1	262	4/4	3	1	–
OSP-2	306	8/7	6	–	1
OSP-3	282	4/3	2	1	–
Total (piglet ID)		16/14	11 (MT01–MT11)	2 (MT12 and MT13)	1 (MT14)

[a] Two *OSBPL2*$^{-/-}$ cell colonies were pooled into one nuclear transfer. MT, mutant.

matched wild-type (WT) piglets were used as controls (WT-BC, $n = 5$; WT-HFD, $n = 5$). The piglets of the WT-HFD and MT-HFD groups were fed with HFD at 2 months old.

The auditory function of *OSBPL2*$^{c.293insT/c.293insT}$ MT pigs was measured by auditory brainstem response (ABR) thresholds in response to click stimuli (0.5–4 kHz) and tone-burst stimuli (2–16 kHz). The tested frequencies corresponded to 80% of the region from the apex of the pig cochlea (Viberg and Canlon, 2007). Before HFD feeding, the 2-month-old MT pigs had ABR thresholds of 55–65 dB SPL *versus* 40–50 dB SPL in age-matched WT controls (Fig. 2A) and produced visualized ABR waveforms (I–V peaks) after exposure to high stimulus intensity (up to 90 dB SPL) (Fig. 2B). Thereafter, the MT pigs fed with BC exhibited elevated ABR threshold shifts over time at each tested frequency, and more severe HL was detected in the MT-HFD group. The WT pigs fed with BC exhibited less varied ARB thresholds after 2 months of age, and there were no remarkable differences in ABR thresholds between the age-matched WT-BC and WT-HFD groups. At 12 months old, no recognizable ABR waveforms could be provoked in MT-BC and MT-HFD pigs until the stimulus intensities reached 90 and 105 dB SPL, respectively (Fig. 2B).

To investigate the pathological effect of *OSBPL2* disruption on auditory function, scanning electron microscopy (SEM) was used to examine the ultrastructure of inner HCs (IHCs) and outer HCs (OHCs) of the 2-month-old *OSBPL2*$^{c.293insT/c.293insT}$ pigs. As shown in Fig. 3, the OHCs, IHCs and their stereocilia were missing at the basal-middle turn of the organ of Corti in 12-month-old MT pigs. Notably, the MT-HFD group exhibited more significant loss or degeneration of OHCs and IHCs than the MT-BC group. Additionally, IHC stereocilia in the MT-HFD group appeared more extensively missing and disorganized than those of the MT-BC group. In contrast, the OHCs and IHCs were intact and morphologically normal in age-matched WT-BC and WT-HFD pigs. The morphologies of auditory HCs were consistent with the ABR threshold shifts in *OSBPL2*$^{c.293insT/c.293insT}$ pigs with or without HFD.

2.4. Effect of OSBPL2 disruption on cell apoptosis in the cochlea

The terminal-deoxynucleotidyl transferase dUTP nick end labeling (TUNEL) staining assay was performed to further investigate the potential pathological changes of cochlea in *OSBPL2*$^{c.293insT/c.293insT}$ pigs (Fig. 4). No significant pathological changes of cochlea were observed in the12-month-old WT-BC and WT-HFD pigs. In 2-month-old MT pigs before HFD feeding, no regions in cochlea were TUNEL-positive except HCs, while extensive TUNEL-positive regions in cochlea, including HCs, stria vascularis (SV) and spiral ganglion (SG), were observed in 12-month-old MT-BC pigs, indicating aggravated apoptosis over time. The 12-month-old MT-HFD pigs also had extensive TUNEL-positive regions in cochlea, while more SV cells were TUNEL-positive than that of the age-matched MT-BC group. These results provided confirmatory evidence of auditory dysfunction, as mentioned above.

2.5. Effect of OSBPL2 disruption on serum lipid profiles

The potential effect of *OSBPL2* disruption on serum lipids was investigated in *OSBPL2*$^{c.293insT/c.293insT}$ and WT pigs fed with or without HFD. The serum lipid levels were determined at varying month ages after 2 months old. Compared with the age-matched WT-BC group, a considerable elevation in triglyceride (TG), total cholesterol (TC), high-density lipoprotein cholesterol (HDL-C) and low-density lipoprotein cholesterol (LDL-C) levels was detected in the MT-BC group (Fig. 5A–D). HFD feeding resulted in dramatically increased TC level in the MT-HFD group compared to the MT-BC group, but no significant difference in TG levels was observed between these two groups (Fig. 5A and B). Among all groups, the MT-HFD group exhibited the most severe hypercholesterolaemia, because it had the highest TC level which was approximately twice that of the WT-HFD group after 4 months of HFD feeding (Fig. 5B). Notably, the LDL-C level of the MT-HFD group was significantly higher than that of the WT-HFD group at each time point tested (Fig. 5D). These lipid profiles were consistent with the HL development and pathological changes in the cochlea in the MT-BC/HFD groups, suggesting that the role of *OSBPL2* implicated in lipid metabolism might be essential for auditory function.

3. Discussion

In our previous work, we identified *OSBPL2* as a DFNA-causal gene (*DFNA67*), a frameshift mutation (c.153_154delCT, p.Gln53Argfs*100) in which completely co-segregated with the phenotype of progressive HL in a large Chinese family (Xing et al., 2015). Coincidently, another frameshift mutation (c.141_142delTG, p.Arg50Alafs*103) was identified in an affected German family and co-segregated with the same clinical phenotype as that of the Chinese family (Thoenes et al., 2015). According to the standards and guidelines for the interpretation of sequence variants developed by the American College of Medical Genetics and Genomics (ACMG) (Richards et al., 2015), these two co-segregating frameshift mutations in *OSBPL2* provided mutual proof and convincing evidence of their pathogenicity for a Mendelian disorder. However, the role of *OSBPL2* in auditory function, especially the genotype-phenotype association, needs to be further investigated.

OSBPL2 has drawn much attention as a sterol sensor and transporter that modulates cell signaling, vesicular trafficking and lipid metabolism (Laitinen et al., 2002; Suchanek et al., 2007; Hynynen et al., 2009; Sewer and Li, 2013; Escajadillo et al., 2016; Kentala et al., 2018a, 2018b). Several OSBP/ORP family members (e.g., OSBP, OSBPL1L, and OSBPL11) have been found to be implicated in some dyslipidaemia-associated diseases (e.g., hepatic lipogenesis, cardiovascular disease and obesity) (Yan et al., 2007a, b; Bouchard et al., 2009), but the identification of *OSBPL2* as an NSHL-causal gene provides new evidence to prompt the hypothesis on the SNHL-dyslipidaemia association. Accumulated epidemiologic studies have suggested that hyperlipidaemia/hypercholesterolaemia could be associated with SNHL development

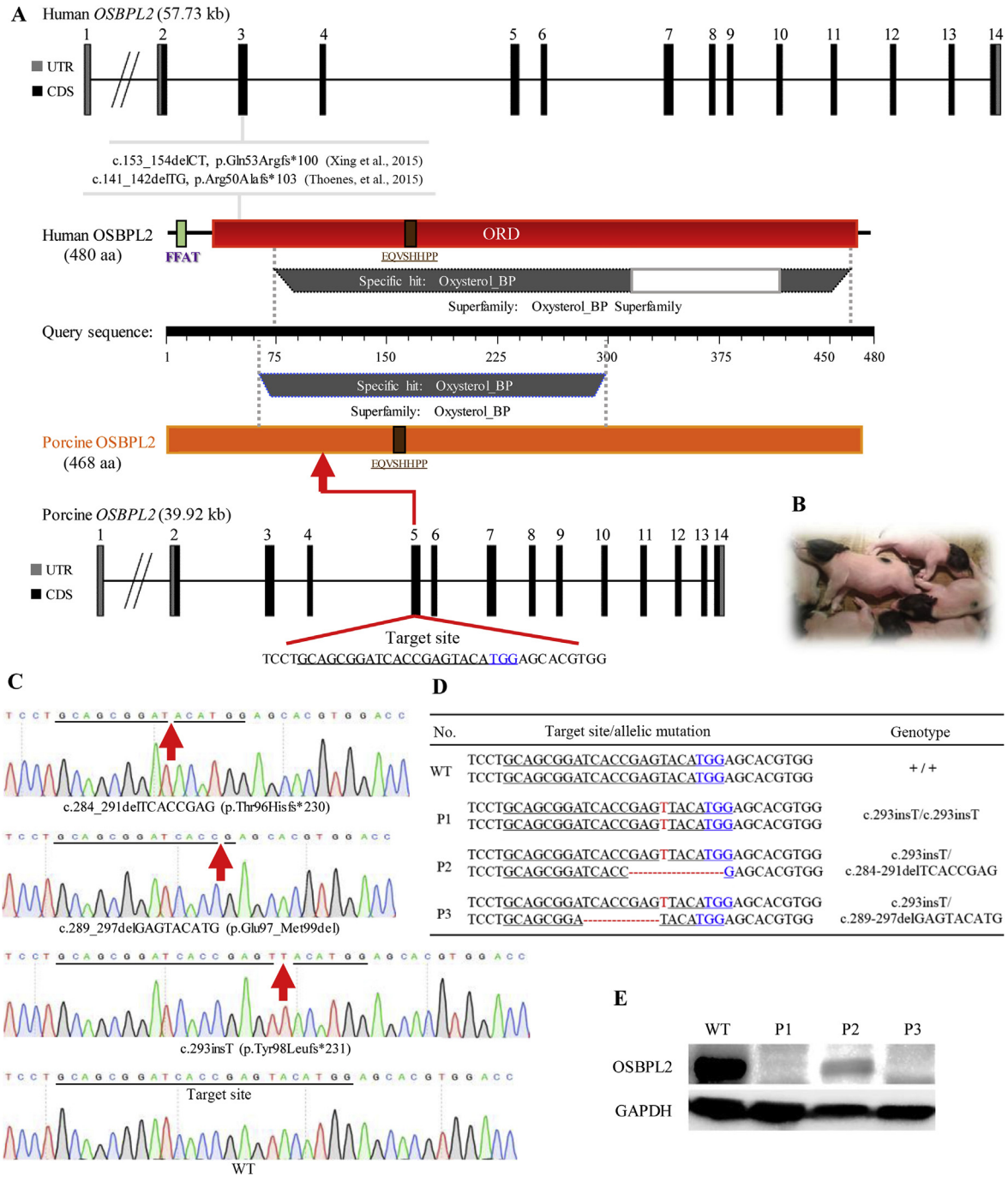

Fig. 1. Schematic representation of experimental design for generating *OSBPL2*-disrupted PFFs and piglets. **A**: Schematic diagram of the gene and protein structures of human and porcine *OSBPL2* as well as the target site of sgRNA-exon5. FFAT, two phenylalanines in an acidic tract motif; ORD, OSBP-related domain; EQVSHHPP, OSBP fingerprint motif. **B**: The image of newborn *OSBPL2*$^{-/-}$ piglets. **C**: Sequencing chromatograms of *OSBPL2* allelic mutations in *OSBPL2*$^{-/-}$ piglets compared with the wild-type (WT) control. The target site is underlined, and the mutated nucleotides are marked by red arrows. **D**: The genotypes of newborn *OSBPL2*$^{-/-}$ piglets. **E**: Western blot analysis of OSBPL2 protein from ear skin biopsies of *OSBPL2*$^{-/-}$ and WT piglets. GAPDH was used as a loading control.

(Evans et al., 2006; Berardino et al., 2007; Helzner et al., 2011; King et al., 2014; Chang et al., 2015; Malgrange et al., 2015; Aghazadeh-Attari et al., 2017). Some genetic syndromes, such as Smith-Lemli-Opitz syndrome and Niemanne-Pick disease (Berardino et al., 2007; King et al., 2014), also indicate the association of cholesterol homeostasis dysregulation with syndromic SNHL. However, there is still a lack of genetic evidence and *de novo* functional assessment to support the linkage of auditory dysfunction and dyslipidaemia/hypercholesterolaemia. *OSBPL2* might be the key to substantiating this linkage. To further elucidate the role of *OSBPL2* in auditory function and lipid metabolism, it is crucial to develop adaptable animal models.

Inbred and genetically modified animal models, such as fruit flies, zebrafish and rodents, have been used to investigate the aetiology and pathogenesis of human HL (Strain, 2015; Zou et al., 2015; Chen et al., 2016). However, these animals insufficiently reflect the pathophysiology of the human inner ear and might not faithfully or expectantly reproduce human genetic HL (Strain, 2015;

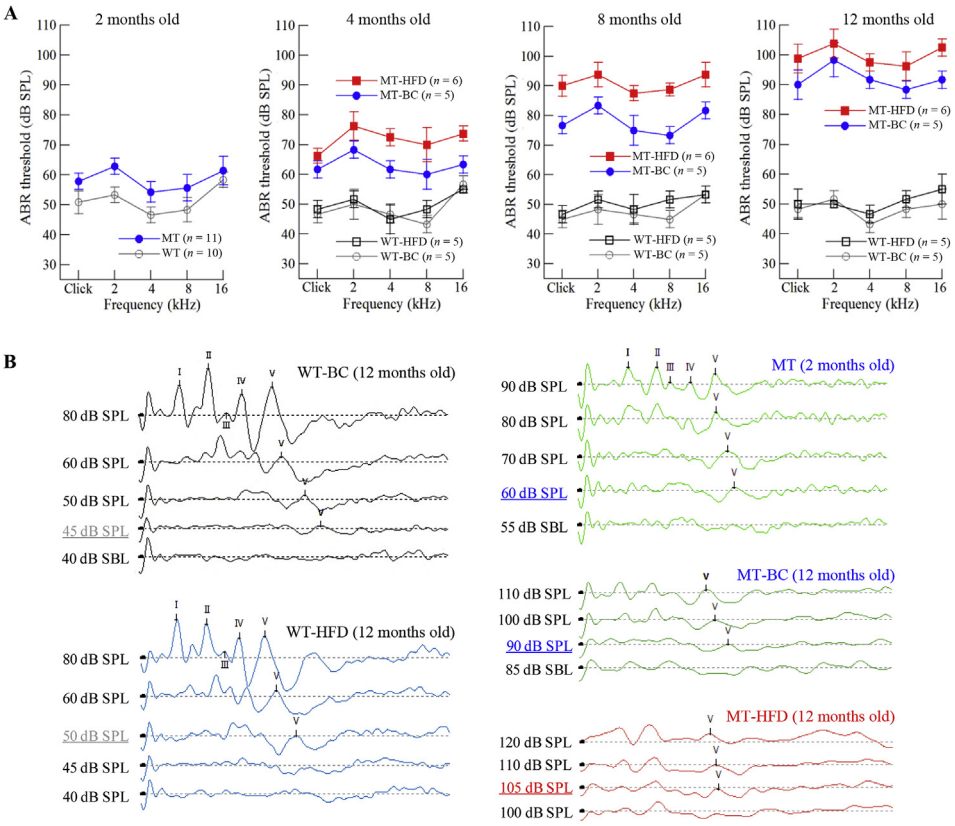

Fig. 2. Evaluation of hearing loss (HL) in *OSBPL2*$^{-/-}$ pigs. **A**: Time course of ABR thresholds in *OSBPL2*$^{-/-}$ mutant (MT) and wild-type (WT) pigs. *OSBPL2*$^{-/-}$ pigs were divided into the basic chow (MT-BC) and high-fat diet (MT-HFD) groups and subjected to subsequent ABR threshold test. Age-matched WT piglets were used as controls. The differences in ABR thresholds between MT-BC and WT-BC, MT-HFD and WT-HFD, and MT-BC and MT-HFD are significant for all tested frequencies ($P < 0.05$, two-tailed Student's *t*-test). The WT-BC pigs exhibited less varied ARB thresholds after 2 months old. HFD hardly affected the hearing function of the WT-HFD group but resulted in more severe HL in MT-HFD pigs than age-matched MT-BC pigs. **B**: Click-evoked ABR waveforms in *OSBPL2*$^{-/-}$ MT and WT pigs. All the ABR traces were recorded at the same measurement range for latency (0–10 ms) and amplitude (0–1 μV).

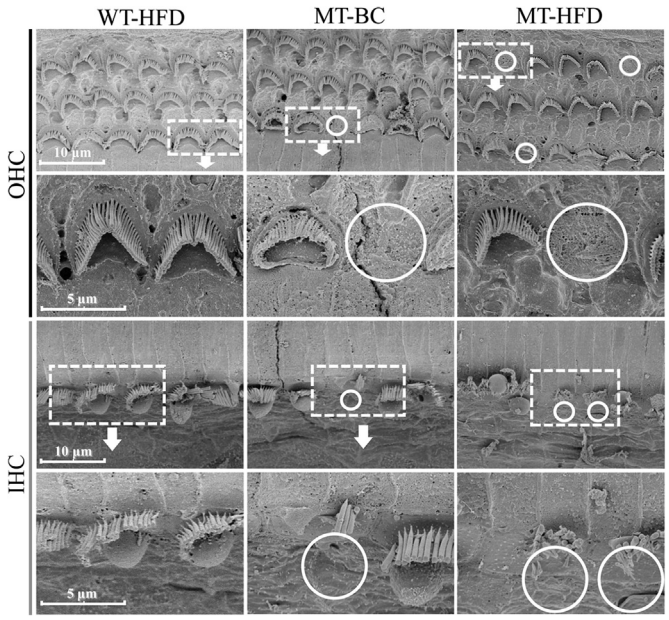

Fig. 3. Scanning electron microscopy (SEM) analysis of inner hair cells (IHCs) and outer hair cells (OHCs) at the basal-middle turn in the cochlea of 12-month-old *OSBPL2*$^{-/-}$ mutant (MT) and wild-type (WT) pigs. White circles denote the regions with OHC/IHC loss or degeneration, and dashed boxes denote the locally zoomed regions with abnormal OHC/IHC morphologies.

Zou et al., 2015). Recently, the completion of the swine genome has provided a platform for discovering putative causal genes for various genetic diseases and contributes to the development of novel disease models (Bendixen et al., 2010; Prabhakar, 2012; Walters et al., 2012; Zhou et al., 2015). Compared with the mouse models currently used in otic research, pig models have a longer lifespan and more similarities to humans in terms of otic size and structure as well as the pathophysiologic characteristics of the inner ear (Lovell and Harper, 2007; Guo et al., 2015; Strain, 2015), which enable detailed characterization and better understanding of the pathologic processes of human HL, especially in the case of late-onset progressive HL. In addition, newborn and adult pigs exhibit indistinguishable hearing with similar hearing frequency and threshold to humans, while newborn and adult mice exhibit differential hearing (Lovell and Harper, 2007; Strain, 2015; Hai et al., 2017b). The genetic, physiologic, anatomic and otic similarities between pigs and humans make pigs a superior model for the investigation of human HL and the development of novel therapeutic agents and treatments (Zhou et al., 2015; Hai et al., 2017a; 2017b; Yao et al., 2017; Yan et al., 2018). With the advent of gene editing and SCNT, it became feasible to generate genetically engineered pigs with the desired genotypes. Chen et al. (2016) and Hai et al. (2017b) created miniature pig models with homozygous and biallelic knockout mutations in the porcine *MITF* gene using ethylnitrosourea (ENU) mutagenesis and CRISPR/Cas9-mediated editing, respectively, which resembled the clinical symptoms and pathology of human Waardenburg syndrome type 2A (WS2A). Considering the highly syntenic and close evolutionary features of

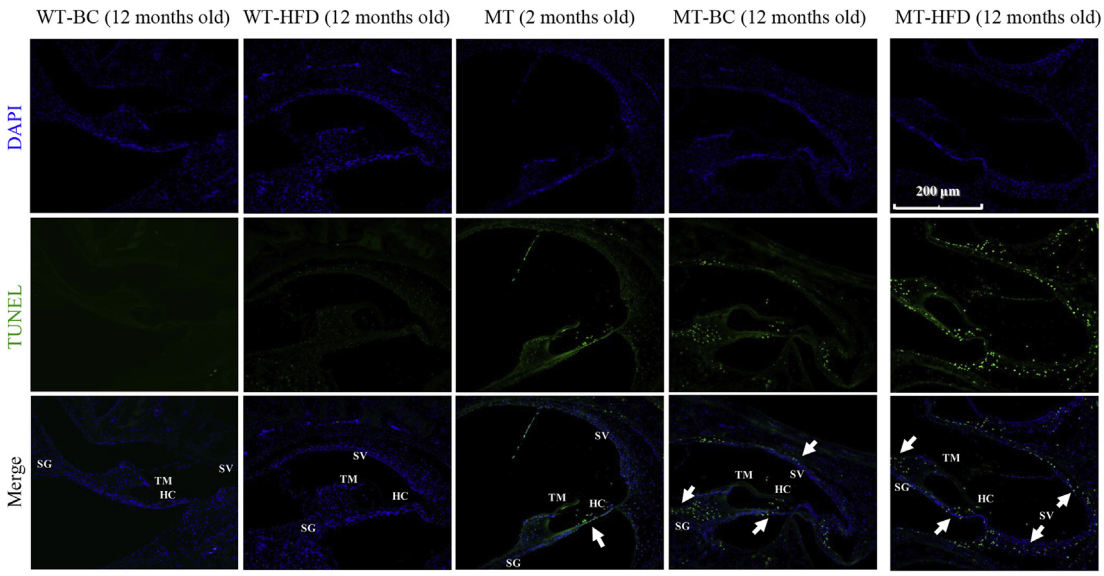

Fig. 4. TUNEL staining of cochleae in *OSBPL2*$^{-/-}$ mutant (MT) and wild-type (WT) pigs. TUNEL-positive signals were observed in the cochleae of the 2-month-old MT pigs and 12-month-old MT-BC/HFD pigs, but not in the cochleae of age-matched WT pigs. Arrows denote the TUNEL-positive regions in the cochlea. HC, hair cell; TM, tectorial membrane; SV, stria vascularis; SG, spiral ganglion.

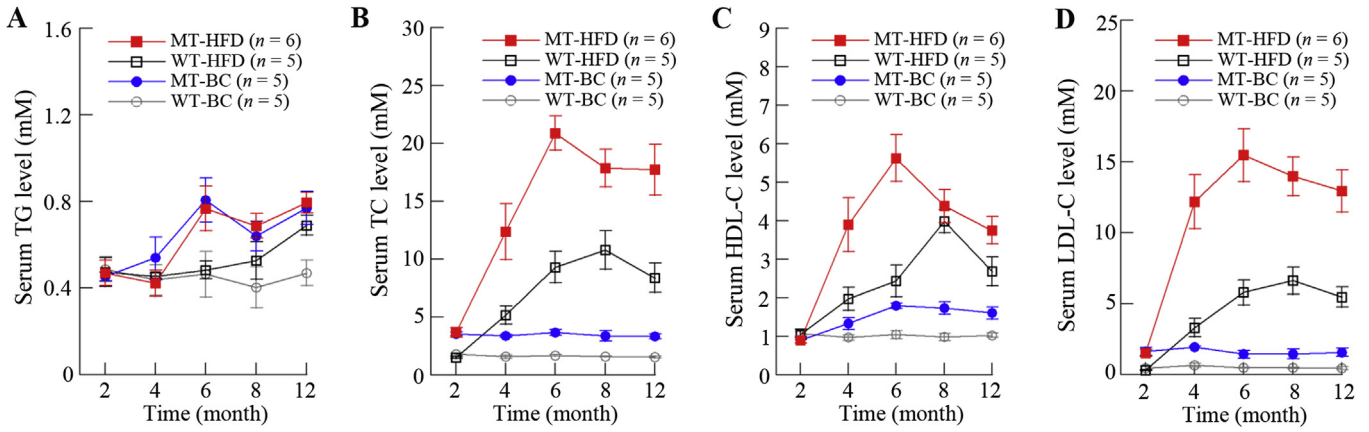

Fig. 5. The serum lipid profiles of *OSBPL2*$^{-/-}$ mutant (MT) and wild-type (WT) pigs. **A**: Serum triglyceride (TG) level. **B**: Serum total cholesterol (TC) level. **C**: Serum high-density lipoprotein cholesterol (HDL-C) level. **D**: Serum low-density lipoprotein cholesterol (LDL-C) level. The differences in TC and LDL-C between MT-BC and WT-BC, MT-HFD and WT-HFD, and MT-BC and MT-HFD are significant at each time point tested ($P < 0.05$, two-tailed Student's *t*-test).

porcine and human *OSBPL2*, the pig model is preferred for the functional assessment of *OSBPL2* disruption. To date, there are no references that have described NSHL-causal genes, including *DFNA*, *DFNB* and *DFN*, in pig models.

CRISPR/Cas9-mediated gene editing provides an efficient and robust approach to resemble human diseases and their underlying causalities by disruption of normal gene alleles in model organisms. In the present study, the CRISPR/Cas9 system was used to construct *OSBPL2*-disrupted PFFs by targeting the conserved ORD region of *OSBPL2*. As we expected, all *OSBPL2*$^{-/-}$ pigs recapitulated dual phenotypes of progressive HL and dyslipidaemia/hypercholesterolaemia (Tables S4 and S5), confirming that *OSBPL2* is essential for auditory function and plays an important role in lipid metabolism. In addition, HFD could lead to aggravated HL and more severe hypercholesterolaemia. It is noteworthy that HFD hardly affected the hearing function of the WT-HFD group but resulted in more severe HL in MT-HFD pigs than age-matched MT-BC pigs. These results suggested that OSBPL2 deficiency is responsible for HL in pig models, which could be synergistically affected by both genetic and environmental factors. The degeneration of OHCs and IHCs and abnormalities of stereocilia as well as apoptosis in cochlea in *OSBPL2*$^{-/-}$ pigs provided conformable results that *OSBPL2* disruption effected auditory function. The dual phenotypes of *OSBPL2*$^{-/-}$ pigs fed with or without HFD suggested that OSBPL2 is essential for maintaining cellular cholesterol homeostasis with optimal cholesterol output and posit, and aberrant expression and/or dysfunction of this lipid binding protein could contribute to disease phenotypes associated with hypercholesterolaemia. In addition to the regulatory roles in cellular lipid homeostasis and metabolism, Kentala et al. (2018a, 2018b) revealed that OSBPL2 could function as a new regulatory nexus in Akt signaling, actin cytoskeleton function, cellular energy metabolism, cell migration, adhesion and proliferation. OSBPL2 was found to be involved in the morphology regulation of F-actin, which could form a key structural element of stereocilia (Kentala et al., 2018a). Considering the prominent expression of *OSBPL2* in cochlea SV, SG, HCs and HC

stereocilia (Xing et al., 2015; Thoenes et al., 2015), we speculated that *OSBPL2* could also play a key role in maintaining the cytoskeleton of cochlea cells. Thus, OSBPL2 disruption could lead to the apoptosis/degeneration of cochlea SV, SG and HCs as well as morphological abnormalities of HC stereocilia, leading to auditory function impairment.

In summary, we successfully created a novel *OSBPL2*-disrupted pig model which exhibited dual phenotypes of progressive HL and hypercholesterolaemia, which faithfully resembled the auditory disorder in affected patients carrying *OSBPL2* mutations. To our knowledge, this is the first time that the NSHL-causal gene was targeted, modified, and functionally assessed in large animal models. This work contributed to understanding the pathogenesis of *OSBPL2* deficiency, which might be the key to elucidating the potential linkage between auditory dysfunction and dyslipidaemia.

4. Materials and methods

4.1. Animals and cell lines

Bama miniature (BM) pigs were purchased from Chia Tai Co., Ltd. (Huaiyin, China) and housed in the animal facility affiliated with Nanjing Medical University (Nanjing, China). All animals were subjected to standard husbandry procedures. The animal use protocol complied with the guidelines of the Institutional Animal Care and Use Committee (IACUC) of Nanjing Medical University. All surgical procedures, including embryo transplantation and auditory test, were conducted under anaesthesia to minimize animal suffering.

Porcine foetal fibroblasts (PFFs) were isolated from the skin of a 1-month-old female BM foetus using 200 U/mL collagenase and 25 kU/mL DNaseI (Invitrogen, USA), cultured in Dulbecco's modified Eagle's medium (10% foetal bovine serum, MEM non-essential amino acids, and 1 mM sodium pyruvate) (DMEM, Invitrogen), and maintained at 37 °C for 48 h in a humidified incubator containing 5% CO_2. The cumulus-oocyte complexes were derived from the ovaries of 6-month-old gilts (Chinese Landrace) at a local abattoir.

4.2. Construction of Cas9-sgRNA vectors and T7E1 cleavage assay

To achieve *OSBPL2* disruption in BM pigs, two single guide RNAs (sgRNAs) were designed using online tools (http://crispr.mit.edu/). The oligos of sgRNAs were synthesized (Genscript, China), and the complementary oligos were annealed to double-stranded DNA and ligated to the *Bbs*I-digested pX330 vector (Addgene plasmid 423230) to generate the Cas9-sgRNA constructs, which were then transfected into PFFs using the Basic Fibroblast Nucleofection Kit (Amaxa Biosystems, Germany). The post-transfected cells were cultured for 48 h as described above and collected for genomic DNA extraction using a DNA extraction kit (TianGen, China). Primers flanking the CRISPR/Cas9-targeting sites were designed based on the porcine genomic sequence (NC_010459.5) and synthesized by BGI-Beijing (Shenzhen, China). The purified PCR products were denatured and annealed to form a heteroduplex. The annealed products were subjected to a T7E1 cleavage assay to assess the cleavage efficiency of sgRNAs (Fang et al., 2018). The sgRNA with higher cleavage efficiency was selected for subsequent gene editing.

4.3. PFF cell selection

The Cas9-sgRNA construct carrying *Cas9* and sgRNA-exon5 and the neomycin-resistant pCMV-td-Tomato plasmid (Clontech, Japan) were co-transfected into 1×10^6 PFFs as mentioned above. The neomycin-resistant colonies were selected using 0.8 mg/mL G418 (Gibco, USA). The single cell colonies were seeded in 48-well plates. After reaching 90% confluency, cells of each colony were passaged to 12-well plates, sub-cultured for 48 h, washed by PBS twice and suspended in 2 mL DMEM. Then, 0.4 mL suspended cells of each colony were lysed in 0.45% NP-40 lysis buffer for 40 min (55 °C, 30 min; 95 °C, 10 min), and the remaining cells were used for somatic cell nuclear transfer (SCNT). Genomic DNA was extracted from the lysate and used for PCR-based screening of positive mutant colonies. The PCR products were ligated to a pMD18-T vector (Clontech), and 15–20 recombinant clones for both alleles were picked and sequenced. The positive mutant colony cells of PFFs were selected as donor cells for SCNT.

4.4. SCNT and embryo transplantation

Porcine oocyte collection, *in vitro* maturation and SCNT were conducted as previous described (Fang et al., 2018). Briefly, the cumulus-oocyte complexes were collected and cultured in TCM-199 maturation medium (Gibco) for 42 h, and then matured oocytes were isolated and enucleated. The donor cells were microinjected into the perivitelline space of the enucleated oocytes. Fusion and activation were conducted using a Voltain EP-1 cell fusion system (Cryologic, Australian). The reconstructed embryos were cultured in embryo-development medium at 38.5 °C for 24 h and then transferred surgically into the oviducts of oestrus-synchronized pig surrogates (each recipient receiving 250–300 embryos). The pregnancy status was examined by ultrasonography 30 days after embryo transfer and monitored weekly until the perinatal period. The cloned piglets were delivered by natural birth.

4.5. Genotyping and Western blot analysis

Genomic DNA and total proteins were extracted from the ear skin biopsies of the cloned piglets. Mutagenesis at the target site of both alleles was assessed via PCR-based sequencing. Potential off-target sites (OTS) (allowing $\leq$6 mismatches within the 20-nt sgRNA and 3-nt protospacer adjacent motif (PAM) sequences) were predicted by CRISPR direct (http://crispr.dbcls.jp/). All OTS were subjected to PCR-based sequencing to assess the off-target effects. Total proteins were extracted using T-PER™ Tissue Protein Extraction Reagent (Thermo Fisher Scientific, USA). The protein samples were separated by 10% SDS-PAGE (Bio-Rad, USA) and transferred onto polyvinylidene fluoride (PVDF) membranes. After blocking with 5% non-fat dry milk in Tris-buffered saline containing 0.05% Tween-20 (TBST) for 3 h at room temperature, PVDF membranes were washed in TBST and incubated with the anti-OSBPL2 goat polyclonal antibody (1:50; Santa Cruz Biotech., USA) overnight. The membranes were washed again and incubated with an HRP-conjugated secondary antibody (1:800; Bioworld, USA) for 2 h at room temperature. The target protein was rinsed with TBST and detected using the enhanced ECL chemiluminescence detection system (Millipore, USA). GAPDH was used as the loading control.

4.6. Animal grouping and sampling

The mutant (MT) and wild-type (WT) piglets were sorted via ear punching. All piglets were fed with basic chow (BC) for 1 month after weaning. At 2 months old, the MT and WT piglets were fed with or without high-fat diet (HFD) and grouped as MT-BC, MT-HFD, WT-BC and WT-HFD, respectively. The BC was commercially purchased from Chia Tai Co., Ltd. The HFD (Xietong Pharmaceutical Bioengineering Co., Ltd., China) was prepared according to the following recipe (w/w): 63.5% BC, 1.5% cholesterol, 15%

oleomargarine, 10% lard and 10% yolk powder. All piglets were monitored daily for general health, and blood was sampled weekly until the end of the experiment. The auditory test was performed monthly. The piglets were finally sacrificed and tissue-sampled under the inhalation anaesthesia of isoflurane and N_2O.

4.7. Auditory test

Auditory brainstem response (ABR) was used to assess the auditory function. The animal was subjected to an intramuscular injection of xylazine (10 mg/kg) and inhalation anaesthesia of isoflurane and mixed N_2O/O_2 (1/3). They were kept warm with a heat pad and placed in a soundproof room. The acoustic stimuli, including click stimuli (0.5–4 kHz) and tone-burst (TB) stimuli (2, 4, 8, and 16 kHz), were evoked using the Neuro-Audio/ABR system (Neurosoft, Russian). The ABR waveforms of evoked potentials were recorded at varying stimulus intensities with 5 dB sound pressure level (SPL) intervals, and the ABR peak V could be visualized at the same latency after an average of 1024 recordings. The ABR thresholds were determined by the lowest stimulus intensity, which could induce the detectable and reproducible ABR peak V ($\geq$0.1 μV). The mean thresholds were verified in triplicate at each frequency.

4.8. Scanning electron microscopy (SEM)

The cochlea was carefully removed from the porcine skull based on the similar methodology described by Guo et al. (2015). The morphology of the porcine cochlea was examined using SEM as previously described (Hai et al., 2017a, 2017b). Briefly, the cochleae were fixed with 2.5% glutaraldehyde in SCB (sodium cacodylate buffer; 0.1 M, pH 7.2) overnight and decalcified with 14% EDTA for 30 days. After removal of the covering bones, the cochlea was cut into sections at each half turn and dissected from the modiolus around the inner edge of the spiral lamina. Each section was placed into 2.5% glutaraldehyde in SCB for 1 h, rinsed twice in SCB for 15 min, and fixed with 1% OsO_4 in SCB for 1 h. The desiccated samples were mounted on aluminium specimen stubs, sputter-coated with gold particles (Emitech K550, UK), and examined using SEM (Hitachi S-3700N, Japan).

4.9. TUNEL staining

The dissected cochleae were fixed in 4% paraformaldehyde overnight, decalcified as mentioned above, dehydrated in gradient ethanol solutions and embedded in paraffin for sectioning. TUNEL staining was conducted using an *In Situ* Cell Death Detection Kit (Roche, USA) according to the manufacturer's protocols. The specimens were embedded in Vectashield mounting medium containing the nuclear marker DAPI (Vector Laboratories, USA), and viewed using a laser scanning confocal microscope (Carl Zeiss LSM710, German).

4.10. Serum lipid assay

Whole blood samples were obtained from the jugular veins of overnight-fasted pigs at the predetermined time. Sera were separated by centrifugation (500 ×*g*) for 15 min at room temperature. The levels of serum lipids, including triglyceride (TG), total cholesterol (TC), high-density lipoprotein cholesterol (HDL-C) and low-density lipoprotein cholesterol (LDL-C), were determined using the BS-230 Biochemical Analyzer (Mindray, China).

4.11. Statistical analysis

All data were presented as mean ± SEM. Statistical analysis was performed using an independent, two-tailed Student's *t*-test. A *P*-value less than 0.05 was considered significantly different.

Acknowledgments

We are grateful to all laboratory staffs of Jiangsu Key Laboratory of Xenotransplantation for their kind help in this project. This work was supported by grants from the National Natural Science Foundation of China (81771000 and 31571302), the Key Research and Development Program of Jiangsu Province (Social Development: BE2016762) and the Key Project of Science and Technology Innovation of Nanjing Medical University (2017NJMUCX001) to X.C., and grants from the China Postdoctoral Science Foundation (2016M600431) and the Jiangsu Planned Projects for Postdoctoral Research Funds (1601071B) to J.Y.

Supplementary data

Supplementary data to this article can be found online at https://doi.org/10.1016/j.jgg.2019.06.006.

References

Aghazadeh-Attari, J., Mansorian, B., Mirza-Aghazadeh-Attari, M., Ahmadzadeh, J., Mohebbi, I., 2017. Association between metabolic syndrome and sensorineural hearing loss: a cross-sectional study of 11,114 participants. Diabetes Metab. Syndr. Obes. 10, 459–465.

Bendixen, E., Danielsen, M., Larsen, K., Bendixen, C., 2010. Advances in porcine genomics and proteomics–a toolbox for developing the pig as a model organism for molecular biomedical research. Brief. Funct. Genomics 9, 208–219.

Berardino, F.D., Alpini, D., Ambrosetti, U., Amadeo, C., Cesarani, A., 2007. Sensorineural hearing-loss in the Smith-Lemli-Opitz syndrome. Int. J. Pediatr. Otorhinolaryngol. Extra 2, 169–172.

Bouchard, L., Faucher, G., Tchernof, A., Deshaies, Y., Marceau, S., Lescelleur, O., Biron, S., Bouchard, C., Perusse, L., Vohl, M.C., 2009. Association of *OSBPL11* gene polymorphisms with cardiovascular disease risk factors in obesity. Obesity 17, 1466–1472.

Chang, I.J., Kang, C.J., Yueh, C.Y., Fang, K.H., Yeh, R.M., Tsai, Y.T., 2015. The relationship between serum lipids and sudden sensorineural hearing loss: a systematic review and meta-analysis. PLoS One 10, e0121025.

Chen, L., Guo, W., Ren, L., Yang, M., Zhao, Y., Guo, Z., Yi, H., Li, M., Hu, Y., Long, X., Sun, B., Li, J., Zhai, S., Zhang, T., Tian, S., Meng, Q., Yu, N., Zhu, D., Tang, G., Tang, Q., Ren, L., Liu, K., Zhang, S., Che, T., Yu, Z., Wu, N., Jing, L., Zhang, R., Cong, T., Chen, S., Zhao, Y., Zhang, Y., Bai, X., Guo, Y., Zhao, L., Zhang, F., Zhao, H., Zhang, L., Hou, Z., Zhao, J., Li, J., Zhang, L., Sun, W., Zou, X., Wang, T., Ge, L., Liu, Z., Hu, X., Wang, J., Yang, S., Li, N., 2016. A *de novo* silencer causes elimination of *MITF-M* expression and profound hearing loss in pigs. BMC Biol. 14, 52.

Cohen, M.M., Gorlin, R.J., 1995. Hereditary hearing loss and its syndromes. In: Gorlin, R.J., Toriello, H.V., Cohen, M.M. (Eds.), Oxford Monographs on Medical Genetics. Oxford University Press, New York, US, pp. 9–21.

Dror, A.A., Avraham, K.B., 2009. Hearing loss: mechanisms revealed by genetics and cell biology. Annu. Rev. Genet. 43, 411–437.

Egilmez, O.K., Kalcioglu, M.T., 2016. Genetics of nonsyndromic congenital hearing loss. Scientifica (Cairo) 2016, 7576064.

Escajadillo, T., Wang, H., Li, L., Li, D., Sewer, M.B., 2016. Oxysterol-related-binding-protein related protein-2 (ORP2) regulates cortisol biosynthesis and cholesterol homeostasis. Mol. Cell. Endocrinol. 427, 73–85.

Evans, M.B., Tonini, R., Shope, C.D., Oghalai, J.S., Jerger, J.F., Insull Jr., W., Brownell, W.E., 2006. Dyslipidemia and auditory function. Otol. Neurotol. 27, 609–614.

Fang, B., Ren, X., Wang, Y., Li, Z., Zhao, L., Zhang, M., Li, C., Zhang, Z., Chen, L., Li, X., Liu, J., Xiong, Q., Zhang, L., Jin, Y., Liu, X., Li, L., Wei, H., Yang, H., Li, R., Dai, Y., 2018. Apolipoprotein E deficiency accelerates atherosclerosis development in miniature pigs. Dis. Model. Mech. 11 pii: dmm036632.

Guo, W., Yi, H., Ren, L., Chen, L., Zhao, L., Sun, W., Yang, S.M., 2015. The morphology and electrophysiology of the cochlea of the miniature pig. Anat. Rec. (Hoboken) 298, 494–500.

Hai, T., Cao, C., Shang, H., Guo, W., Mu, Y., Yang, S., Zhang, Y., Zheng, Q., Zhang, T., Wang, X., Liu, Y., Kong, Q., Li, K., Wang, D., Qi, M., Hong, Q., Zhang, R., Wang, X., Jia, Q., Wang, X., Qin, G., Li, Y., Luo, A., Jin, W., Yao, J., Huang, J., Zhang, H., Li, M., Xie, X., Zheng, X., Guo, K., Wang, Q., Zhang, S., Li, L., Xie, F., Zhang, Y., Weng, X., Yin, Z., Hu, K., Cong, Y., Zheng, P., Zou, H., Xin, L., Xia, J., Ruan, J., Li, H., Zhao, W., Yuan, J., Liu, Z., Gu, W., Li, M., Wang, Y., Wang, H., Yang, S., Liu, Z., Wei, H., Zhao, J., Zhou, Q., Meng, A., 2017. A pilot study of large-scale production of

mutant pigs by ENU mutagenesis. eLife 6, e26248.
Hai, T., Guo, W., Yao, J., Cao, C., Luo, A., Qi, M., Wang, X., Wang, X., Huang, J., Zhang, Y., Zhang, H., Wang, D., Shang, H., Hong, Q., Zhang, R., Jia, Q., Zheng, Q., Qin, G., Li, Y., Zhang, T., Jin, W., Chen, Z.Y., Wang, H., Zhou, Q., Meng, A., Wei, H., Yang, S., Zhao, J., 2017. Creation of miniature pig model of human Waardenburg syndrome type 2A by ENU mutagenesis. Hum. Genet. 136, 1463–1475.
Helzner, E.P., Patel, A.S., Pratt, S., Sutton-Tyrrell, K., Cauley, J.A., Talbott, E., Kenyon, E., Harris, T.B., Satterfield, S., Ding, J., Newman, A.B., 2011. Hearing sensitivity in older adults: associations with cardiovascular risk factors in the health, aging and body composition study. J. Am. Geriatr. Soc. 59, 972–979.
Hynynen, R., Suchanek, M., Spandl, J., Bäck, N., Thiele, C., Olkkonen, V.M., 2009. OSBP related protein 2 (ORP2) is a sterol receptor on lipid droplets that regulates the metabolism of neutral lipids. J. Lipid Res. 50, 1305–1315.
Kentala, H., Koponen, A., Kivelä, A.M., Andrews, R., Li, C., Zhou, Y., Olkkonen, V.M., 2018a. Analysis of *ORP2*-knockout hepatocytes uncovers a novel function in actin cytoskeletal regulation. FASEB J. 32, 1281–1295.
Kentala, H., Koponen, A., Vihinen, H., Pirhonen, J., Liebisch, G., Pataj, Z., Kivelä, A., Li, S., Karhinen, L., Jääskeläinen, E., Andrews, R., Meriläinen, L., Matysik, S., Ikonen, E., Zhou, Y., Jokitalo, E., Olkkonen, V.M., 2018b. OSBP-related protein-2 (ORP2): a novel Akt effector that controls cellular energy metabolism. Cell. Mol. Life Sci. 75, 4041–4057.
King, K.A., Gordon-Salant, S., Yanjanin, N., Zalewski, C., Houser, A., Porter, F.D., Brewer, C.C., 2014. Auditory phenotype of Niemann-Pick disease, type C1. Ear Hear. 35, 110–117.
Korver, A., Smith, R.J., Van Camp, G., 2017. Congenital hearing loss. Nat. Rev. Dis. Primers 3, 16094.
Laitinen, S., Lehto, M., Lehtonen, S., Hyvärinen, K., Heino, S., Lehtonen, E., Ehnholm, C., Ikonen, E., Olkkonen, V.M., 2002. ORP2, a homolog of oxysterol binding protein, regulates cellular cholesterol metabolism. J. Lipid Res. 43, 245–255.
Lovell, J.M., Harper, G.M., 2007. The morphology of the inner ear from the domestic pig (*Sus scrofa*). J. Microsc. 228 (Pt 3), 345–357.
Malgrange, B., Varela-Nieto, I., de Medina, P., Paillasse, M.R., 2015. Targeting cholesterol homeostasis to fight hearing loss: a new perspective. Front. Aging Neurosci. 7, 3.
Petersen, M.B., 2002. Non-syndromic autosomal-dominant deafness. Clin. Genet. 62, 1–13.
Prabhakar, S., 2012. Translational research challenges: finding the right animal models. J. Investig. Med. 60, 1141–1146.
Prather, R.S., Lorson, M., Ross, J.W., Whyte, J.J., Walters, E., 2013. Genetically engineered pig models for human diseases. Annu. Rev. Anim. Biosci. 1, 203–219.
Richards, S., Aziz, N., Bale, S., Bick, D., Das, S., Gastier-Foster, J., Grody, W.W., Hegde, M., Lyon, E., Spector, E., Voelkerding, K., Rehm, H.L., ACMG Laboratory Quality Assurance Committee, 2015. Standards and guidelines for the interpretation of sequence variants: a joint consensus recommendation of the American College of Medical Genetics and Genomics and the Association for Molecular Pathology. Genet. Med. 17, 405–424.
Sewer, M.B., Li, D., 2013. Regulation of adrenocortical steroid hormone production by RhoA-diaphanous 1 signaling and the cytoskeleton. Mol. Cell. Endocrinol. 371, 79–86.
Sheffield, A.M., Smith, R.J.H., 2018. The epidemiology of deafness. Cold Spring Harb. Perspect. Med. pii: a033258.
Strain, G.M., 2015. The genetics of deafness in domestic animals. Front. Vet. Sci. 2, 29.
Suchanek, M., Hynynen, R., Wohlfahrt, G., Lehto, M., Johansson, M., Saarinen, H., Radzikowska, A., Thiele, C., Olkkonen, V.M., 2007. The mammalian oxysterol-binding protein-related proteins (ORPs) bind 25-hydroxycholesterol in an evolutionarily conserved pocket. Biochem. J. 405, 473–480.
Thoenes, M., Zimmermann, U., Ebermann, I., Ptok, M., Lewis, M.A., Thiele, H., Morlot, S., Hess, M.M., Gal, A., Eisenberger, T., Bergmann, C., Nürnberg, G., Nürnberg, P., Steel, K.P., Knipper, M., Bolz, H.J., 2015. *OSBPL2* encodes a protein of inner and outer hair cell stereocilia and is mutated in autosomal dominant hearing loss (*DFNA67*). Orphanet J. Rare Dis. 10, 15.
Viberg, A., Canlon, B., 2007. The guide to plotting a cochleogram. Hear. Res. 197, 1–10.
Walters, E.M., Wolf, E., Whyte, J.J., Mao, J., Renner, S., Nagashima, H., Kobayashi, E., Zhao, J., Wells, K.D., Critser, J.K., Riley, L.K., Prather, R.S., 2012. Completion of the swine genome will simplify the production of swine as a large animal biomedical model. BMC Med. Genomics 5, 55.
Xing, G., Yao, J., Wu, B., Liu, T., Wei, Q., Liu, C., Lu, Y., Chen, Z., Zheng, H., Yang, X., Cao, X., 2015. Identification of *OSBPL2* as a novel candidate gene for progressive nonsyndromic hearing loss by whole-exome sequencing. Genet. Med. 17, 210–218.
Yan, D., Lehto, M., Rasilainen, L., Metso, J., Ehnholm, C., Yla-Herttuala, S., Jauhiainen, M., Olkkonen, V.M., 2007a. Oxysterol binding protein induces upregulation of SREBP-1c and enhances hepatic lipogenesis. Arterioscler. Thromb. Vasc. Biol. 27, 1108–1114.
Yan, D., Jauhiainen, M., Hildebrand, R.B., Willems van Dijk, K., Van Berkel, T.J., Ehnholm, C., Van Eck, M., Olkkonen, V.M., 2007b. Expression of human OSBP-related protein 1L in macrophages enhances atherosclerotic lesion development in LDL receptor-deficient mice. Arterioscler. Thromb. Vasc. Biol. 27, 1618–1624.
Yan, S., Tu, Z., Liu, Z., Fan, N., Yang, H., Yang, S., Yang, W., Zhao, Y., Ouyang, Z., Lai, C., Yang, H., Li, L., Liu, Q., Shi, H., Xu, G., Zhao, H., Wei, H., Pei, Z., Li, S., Lai, L., Li, X.J., 2018. A huntingtin knockin pig model recapitulates features of selective neurodegeneration in Huntington's disease. Cell 173, 989–1002.e13.
Yao, X., Wang, X., Liu, J., Hu, X., Shi, L., Shen, X., Ying, W., Sun, X., Wang, X., Huang, P., Yang, H., 2017. CRISPR/Cas9-mediated precise targeted integration *in vivo* using a double cut donor with short homology arms. EBioMedicine 20, 19–26.
Zhou, X., Xin, J., Fan, N., Zou, Q., Huang, J., Ouyang, Z., Zhao, Y., Zhao, B., Liu, Z., Lai, S., Yi, X., Guo, L., Esteban, M.A., Zeng, Y., Yang, H., Lai, L., 2015. Generation of CRISPR/Cas9-mediated gene-targeted pigs via somatic cell nuclear transfer. Cell. Mol. Life Sci. 72, 1175–1184.
Zou, B., Mittal, R., Grati, M., Lu, Z., Shu, Y., Tao, Y., Feng, Y., Xie, D., Kong, W., Yang, S., Chen, Z.Y., Liu, X., 2015. The application of genome editing in studying hearing loss. Hear. Res. 327, 102–108.